

Lagrangian Perturbation Theory for Biased Tracers: Significance of the Number Conservation

PETER ESPENSHADE ¹ AND JAIYUL YOO ^{1,2}

¹Center for Theoretical Astrophysics and Cosmology, Department of Astrophysics, University of Zürich, Winterthurerstrasse 190, CH-8057, Zürich, Switzerland

²Department of Physics, University of Zürich, Winterthurerstrasse 190, CH-8057, Zürich, Switzerland

ABSTRACT

The Lagrangian perturbation theory provides a simple yet powerful way of computing the nonlinear matter power spectrum, and it has been applied to biased tracers such as halos and galaxies. The number conservation of matter particles allows a simple relation between the fluctuations at the initial and the late times, which is essential in deriving the exact expression for the nonlinear matter power spectrum. Here we investigate the significance of the number conservation in the Lagrangian perturbation theory for biased tracers. We use N -body simulations to test the significance of number conservation by tracing dark matter halo samples in time. For the mass bin sample $\Delta \log M_h (h^{-1} M_\odot) = 0.5$ at $z \simeq 3$, the theoretical predictions for the halos overestimates the power spectrum at $z = 0$ by a factor of three, while the simulation results match the theoretical predictions if the number conservation of halos is imposed in the simulations throughout the evolution. Starting with a halo sample at $z = 0$ as another test, we trace back in time the particles that belong to the halos at $z = 0$ and use their center-of-mass positions as halo positions at $z > 0$. The halo power spectra at $z > 0$ from the simulations agree with the theoretical predictions of the Lagrangian perturbation theory. This numerical experiment proves that the number conservation is crucial in the Lagrangian perturbation theory predictions. We discuss the implications for various applications of the Lagrangian perturbation theory for biased tracers.

1. INTRODUCTION

The Lagrangian perturbation theory offers a framework to trace the matter distribution from early time to present days (Zel'dovich 1970; see also Buchert 1992; Bouchet et al. 1992; Buchert & Ehlers 1993; Buchert 1994; Bouchet et al. 1995; Catelan 1995; Bernardeau et al. 2002). Following the pioneering work by Crocce & Scoccimarro (2006); Matsubara (2008a), it has become an indispensable tool in modeling the bulk motion and the subsequent resummation of the perturbative contributions. More importantly, the Lagrangian perturbation theory provides a simple, but at the same time very powerful way of computing the nonlinear matter power spectrum (Schneider & Bartelmann 1995; Taylor & Hamilton 1996; Matsubara 2008a):

$$P_m(k, t) = \int d^3q e^{-i\mathbf{k}\cdot\mathbf{q}} \langle e^{-i\mathbf{k}\cdot\Delta\Psi} \rangle, \quad (1)$$

where we have ignored the Dirac delta function at $k = 0$, $\Delta\Psi \equiv \Psi(\mathbf{q}_1, t) - \Psi(\mathbf{q}_2, t)$, $\mathbf{q} \equiv \mathbf{q}_1 - \mathbf{q}_2$, and Ψ is the displacement field from the Lagrangian position \mathbf{q} at initial time t_i to the Eulerian position at late time t

$$\mathbf{x}(\mathbf{q}, t) = \mathbf{q} + \Psi(\mathbf{q}, t). \quad (2)$$

These are comoving coordinates (not physical coordinates). The expression for the nonlinear matter power spectrum in Equation (1) is fully exact (see, e.g., Taruya & Colombi 2017; Pietroni 2018; McDonald & Vlah 2018; Rampf et al. 2021). Hence the task of computing the nonlinear matter power spectrum in practice boils down to computing the multi-point correlation functions for the displacement field in Fourier space up to a desired order in perturbations (Taylor & Hamilton 1996; Matsubara 2008a,b; Carlson et al. 2013; Vlah et al. 2015a).

The critical element in the derivation is the conservation of matter particles

$$n_m(\mathbf{x}, t) dV = n_m(\mathbf{q}, t_i) dV_i, \quad (3)$$

where $dV = a^3(t) d^3x$ and $dV_i = a^3(t_i) d^3q$ are the physical volumes at times t and t_i with the corresponding scale factors $a(t)$ and $a(t_i)$ occupied by matter particles, subject to the relation in Equation (2). Since the background physical number density decreases $\bar{n}_m \propto 1/a^3$ (or the comoving number density is constant in time), the conservation equation (3) becomes

$$[1 + \delta_m(\mathbf{x}, t)] d^3x = [1 + \delta_m(\mathbf{q}, t_i)] d^3q, \quad (4)$$

and accounting for the change in the comoving volume factor, we obtain

$$1 + \delta_m[\mathbf{x}(\mathbf{q}, t), t] = \int d^3q' \delta^D[\mathbf{x}(\mathbf{q}, t) - \mathbf{q}' - \Psi(\mathbf{q}', t)] \quad (5)$$

where the fluctuation $\delta_m(\mathbf{q}, t_i)$ at t_i is assumed zero by considering only the growing mode and setting the initial time t_i to be sufficiently early. The matter density fluctuation can then be written in Fourier space as

$$\delta_m(\mathbf{k}, t) = \int d^3q e^{-i\mathbf{k}\cdot(\mathbf{q}+\Psi)}, \quad (6)$$

which then allows one to write the exact expression for the matter power spectrum in Equation (1). Again, the $k = 0$ mode is ignored in Equation (6).

The Lagrangian perturbation theory has been applied to biased tracers (or halos) (Matsubara 2008b; Padmanabhan & White 2009; Matsubara 2011; Carlson et al. 2013; White 2014), and the only change in the above equations is that we cannot set the fluctuation $\delta_h(\mathbf{q}, t_i)$ zero at t_i :

$$[1 + \delta_h(\mathbf{x}, t)] d^3x = [1 + \delta_h(\mathbf{q}, t_i)] d^3q, \quad (7)$$

as the biased tracers form in more biased density peaks at early time, while the matter fluctuations are more homogeneous. However, the key and often understated ingredient about the application of the Lagrangian perturbation theory to biased tracers is the same number conservation, such that the background number density of the biased tracers evolves as the matter particles, such that the background physical number density of the biased tracers evolves as the matter particles,

$$\bar{n}_h \propto 1/a^3 \propto \bar{n}_m, \quad (8)$$

or again the comoving number density of the biased tracers is constant in time. In fact, dark matter halos as the simplest biased tracer evolve through regular mergers with other dark matter halos and continuous accretion of smooth matter components, invalidating Equation (8). Halo mergers account for $\approx 60\%$ of the total halo mass growth for halo masses spanning the range $10^9 M_\odot$ to $10^{14} M_\odot$ and over the redshift range $1 < z < 3$ (Mo & White 1996; Sheth & Tormen 1999a; Tinker et al. 2008, 2010). Large-scale galaxy surveys also showed that the redshift evolution of the mean number density of various galaxy samples is different from the matter component with a constant comoving number density in time or redshift (see, e.g., Eisenstein et al. 2001; White et al. 2011; Brammer et al. 2011; Conselice et al. 2016). Without the number conservation in Equation (8) and hence Equation (7), one cannot obtain the powerful Equation (13) for biased tracers, like Equations (1) and (6) for matter.

In general, this violation of the number conservation for dark matter halos poses no problem in the Lagrangian perturbation theory for biased tracers, as the halo number density $n_h(\mathbf{q}, t_i)$ at early time can represent not the physical number density of those halos identified at t_i , but the spatial distribution of the dark matter particles at t_i that form the halos later in the Eulerian frame, despite the explicit notation $n_h(\mathbf{q}, t_i)$. Hence the number of halos remains unchanged throughout the evolution, while those halos at t_i cannot be physically identified as distinct halos. For dark matter particles, in contrast, Equation (3) represents literally the number conservation throughout the evolution. In practice, the Lagrangian perturbation theory for biased tracers is applied to the halo samples in the Eulerian frame with marginalization of unknown bias parameters, but Equation (7) remains critical in applying the Lagrangian perturbation theory for biased tracers.

Here we use dark matter halos in numerical simulations to quantify how significant the number conservation is in the Lagrangian perturbation theory predictions for biased tracers in terms of describing the evolution of dark matter halos and its clustering. In particular, we first identify dark matter halos at high redshift to extract the Lagrangian bias parameters from the simulations, and we trace the physical evolution of those halos in the simulations to compute the Eulerian bias parameters at redshift zero. The Eulerian bias parameters from the simulations are then compared to the Lagrangian perturbation theory predictions based on the Lagrangian bias parameters from the simulations. We find that the Lagrangian perturbation theory predictions match the numerical simulations, only if the halos number conservation is satisfied. We discuss the implication of our findings for the applications of the Lagrangian perturbation theory in practice in Section 4.

2. BIASED TRACERS

2.1. Lagrangian Perturbation Theory for Biased Tracers

Given the concise and powerful expression for the exact nonlinear matter power spectrum in the Lagrangian perturbation theory, the formalism has been applied to biased tracers (Matsubara 2008b; Padmanabhan & White 2009; Matsubara 2011; Carlson et al. 2013; White 2014). With the number conservation for biased tracers, Equations (4) and (7) can be used in the Lagrangian perturbation theory to model the fluctuation δ_h for biased tracers (or halos) at late time

$$1 + \delta_h[\mathbf{x}(\mathbf{q}, t), t] = [1 + \delta_h(\mathbf{q}, t_i)] \left\{ 1 + \delta_m[\mathbf{x}(\mathbf{q}, t), t] \right\} \quad (9)$$

where we used Equation (5) for the Jacobian.

Expanding the relation in Equation (9) to the linear order in perturbations, we obtain the well-known relation of the Eulerian bias to the Lagrangian bias factor

$$b_1 = 1 + b_1^L, \quad (10)$$

where we defined the bias parameters as

$$\delta_h(\mathbf{x}, t) = b_1 \delta_m(\mathbf{x}, t), \quad \delta_h(\mathbf{q}, t_i) = b_1^L \delta_m^{(1)}(\mathbf{q}, t), \quad (11)$$

in terms of the nonlinear matter fluctuation δ_m for the Eulerian bias and the linear matter fluctuation $\delta_m^{(1)}$ extrapolated to late times for the Lagrangian bias. These bias parameters are the key predictions in the Lagrangian perturbation theory that will be tested against numerical simulations. The bias parameters can be further expanded to include higher order corrections, the tidal tensor bias (Szalay 1988; Fry & Gaztanaga 1993; Catelan et al. 2000; Ma & Fry 2000; Baldauf et al. 2012), as in the effective field theory approach (Mirbabayi et al. 2015; Senatore 2015; Vlah et al. 2015b; Ivanov et al. 2020). Here we restrict our investigation to the linear order in perturbations and defer further in-depth investigations of higher order corrections to future work.

2.2. Numerical Modeling of Biased Tracers

Here we present our numerical methods to track the evolution of biased tracers from early time to late time. We ran ten dark matter-only PKDGRAV3 (Potter et al. 2017) simulations with 2048^3 particles in an $800 h^{-1}\text{Mpc}$ periodic box and $51 h^{-1}\text{kpc}$ softening length yielding a $5.2 \times 10^9 h^{-1}M_\odot$ particle mass. We supplied PKDGRAV3 with the transfer function computed using the Boltzmann solver CLASS (Blas et al. 2011), and we used the second-order Lagrangian perturbation theory initial conditions at starting redshift $z = 49$. We adopt the ΛCDM parameters: dark matter density $\Omega_{\text{DM}} = 0.27$, baryon density $\Omega_b = 0.049$, Hubble constant $h = 0.67$, scalar spectral index $n_s = 0.97$, and primordial power spectrum amplitude $\ln(10^{10}A_s) = 3.0$, consistent with the Planck results (PLANCK Collaboration 2020).

We use our simulation data to identify dark matter halos as biased tracers by using the friends-of-friends algorithm (Davis et al. 1985) implemented in nbodykit (Hand et al. 2018) with linking length $b = 0.2$. We require that each halo be composed of at least 100 particles (or the minimum mass). The halo catalogs are created at each redshift, starting from $z = 2.9$ until $z = 0$, in units of $\Delta z \sim 0.5$, and each dark matter particle is tagged with a unique identification number, such that we can trace which halo individual particles belong to and thereby how halos at one redshift evolve to the next redshift.

In particular, we focus on a halo sample at early time $z_\star = 2.9$ and study how this halo sample evolves forward in time to $z = 0$. Note, however, that $z_\star = 2.9$ is not the initial time t_i in the Lagrangian space, but an intermediate time to infer the bias evolution at $z = 0$. We do not consider higher redshift because we need a large number of halos to ensure that their power spectra are not dominated by shot noise. At z_\star , we consider a halo sample of mass $6.6 \times 10^{11} \leq M(h^{-1}M_\odot) < 2.1 \times 10^{12}$ that contains 60% of halos with the remaining

30% halos below and 10% halos above the halo mass bin, according to the halo mass function (Tinker et al. 2010). At $z = 0$, we consider a halo sample of mass $5.0 \times 10^{13} \leq M(h^{-1}M_\odot) < 5.0 \times 10^{14}$, of which the bias parameter is about two, representing massive galaxies.

To quantify the significance of the number conservation in the Lagrangian perturbation theory predictions for biased tracers, we compute the power spectra P_h of the halo samples at $z = 0$ (or z_\star) from simulations and compare to the predictions based on the bias parameter obtained from the simulations at z_\star (or $z = 0$). The Eulerian bias parameter b_1 at $z = 0$ is related to the Eulerian bias parameter b_1 at z_\star as (Fry 1996; Tegmark & Peebles 1998; Desjacques et al. 2018)

$$b_1(z = 0) = 1 + [b_1(z_\star) - 1] \frac{D(z_\star)}{D(z = 0)}, \quad (12)$$

where $z_\star = 2.9$, and D is the linear growth function. This equation is derived from Equation (9) at linear order in perturbations, bypassing the need to compute b_1^L at the initial time t_i . We compute the bias parameters from numerical simulations by using $b_1(z) = \sqrt{P_h(z)/P_m(z)}$ over $k \leq 0.03 h \text{ Mpc}^{-1}$.

2.3. How Do Halos Evolve through Mergers?

Dark matter halos evolve via numerous mergers with other halos and continuous accretion of mass, such that unlike dark matter particles the identities of halos are rather difficult to track through their evolution. For example, the standard method (or the standard merger tree) finds the most massive progenitor of a given halo from the previous output time in a numerical simulation and assigns its identity to the given halo (Benson et al. 2000; Springel et al. 2001; Croton et al. 2006; Kauffmann et al. 1999). Consequently, when two halos merge into one, a lower-mass halo loses its identity in the standard merger tree. The reality is much more complicated, but this simple scheme makes physical sense when the mass ratio is large.

The critical element in the Lagrangian perturbation theory for biased tracers is that the number of halos is conserved. In the standard approach, the number conservation of halos is achieved at high redshift z by considering dark matter particles that belong to a halo at $z = 0$ as a distinct halo at z , no matter how much they are spread in space or physically unbound. Here we first consider different but more physically motivated ways to achieve the halo number conservation. We construct a *number-conserving* merger tree, in which we start with a sample of halos at z_\star and keep their identities throughout the evolution, even if they merge into a halo of larger mass, no matter how large it is. In case of a merger of two halos with identities we keep, we consider the merged halo as two individual halos at the same position

(double counting). In addition, we consider a slight variation of the number-conserving merger tree and construct a *nearly number-conserving* merger tree by not double counting in the number-conserving merger tree.

In short, given a halo sample at z_* , we construct three different halo samples at $z = 0$ by following the halos according to three different identification schemes. Compared to the standard approach, halo samples according to the number-conserving merger tree are more physically traced in time, though once merged into a bigger halo, they cannot be identified as physically distinct halos either. The number of halos, however, remains the same throughout the evolution. In contrast, a halo sample at $z = 0$ obtained by following the standard merger tree is significantly reduced in number, as many halos in the sample are incorporated into other larger halos by $z = 0$. The crucial difference in three different halo samples is the validity of the number conservation.

Furthermore, we also test the significance of the number conservation in the standard approach to the Lagrangian perturbation theory by identifying dark matter particles in the halo sample at $z = 0$ and tracing those particles backward in time. While those particles at $z > 0$ are not physically bound, we treat those particles as if they form a distinct halo and we use their center of mass as the halo position at $z > 0$ in measuring their power spectrum. In this way, the halo number is also conserved throughout the evolution backward in time.

3. COMPARISON TO NUMERICAL SIMULATIONS

We are now ready to quantify how significant the number conservation is in the Lagrangian perturbation theory for biased tracers. It will be addressed with two separate questions: how badly is the number conservation of halos violated? and how well do the Lagrangian perturbation theory predictions for halos match the halo power spectra in simulations? The implication for its applications in practice will be addressed in Section 4.

First, we investigate how badly the number conservation of halos is violated through mergers, and Figure 1 shows how halos evolve in time. Consider a halo sample in a narrow mass bin $6 \times 10^{11} \leq M(h^{-1}M_\odot) < 2 \times 10^{12}$ at $z_* = 2.9$ shown in the dark gray band, and the halos in the sample grow in mass via accretion and merger in time. According to the standard merger tree, the distribution of this halo sample at $z = 0$ is shown as the dotted curve. The total number of halos in the sample at z_* is reduced by 89% at $z = 0$, as the halos in the sample merge with larger halos and they lose their identity. Furthermore, their mass distribution today is broader than the initial mass range at z_* . The same exercise can be performed backward in time. Consider a halo sample in a narrow mass bin $5 \times 10^{13} \leq M(h^{-1}M_\odot) < 5 \times 10^{14}$ at $z = 0$ shown in the light gray band, which can be representative of an observed galaxy sample today. Accord-

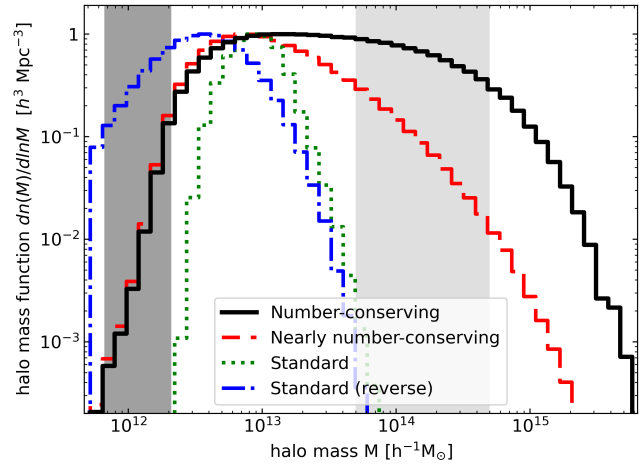


Figure 1. Evolution of halos from a mass-bin sample. Halos in the mass-bins sample (dark gray band) at $z_* = 2.9$ are followed forward in time. The curves are normalized to unity to facilitate the comparison. The standard merger tree (dotted) at $z = 0$ shows that halos at z_* grow in mass, but most (89%) of them disappeared by becoming part of larger mass halos via merger. In contrast, if we keep tracking halos at z_* even when they merge with larger halos, or they merge with each other, the number-conserving merger tree (solid; see text) at $z = 0$ shows that the halos in the narrow mass bin (dark gray band) at z_* are spread over a large range of mass in halos. The nearly-number-conserving merger tree (dashed; see text) shows the change in the halo distribution from the solid curve if we prevent double counting. In the same way, the standard merger tree can be used to trace back the progenitors at z_* (dot-dashed) from the sample at $z = 0$ (light gray band).

ing to the standard merger tree, the distribution of this halo sample at early time z_* is shown as the dot-dashed curve. The progenitor halos that make up the light gray band today originate from a very broad distribution in mass at early time (1.1% of the progenitors at z_* are below the mass resolution). Similar trends are observed across halo samples of different mass. This simple exercise confirms the well-established fact that halos are not static, identical objects throughout the evolution like dark matter particles, but evolving, number-conservation-violating objects that change their properties like mass and shape via mergers and accretions. Of course, galaxies with various observable properties follow much more complicated evolutionary tracks.

To test the significance of the number conservation in the Lagrangian perturbation theory for biased tracers, we construct a halo sample by artificially imposing the number conservation of halos and tracking their evolution from z_* to $z = 0$. Solid and dashed curves in Figure 1 illustrate the halo distributions at $z = 0$ from the halo sample at z_* in the dark gray band, according to the number-conserving (solid) and the nearly number-conserving (dashed) schemes, in which we always keep the identities of the progenitor halos, even when they merge into a larger halo. Consequently, two or

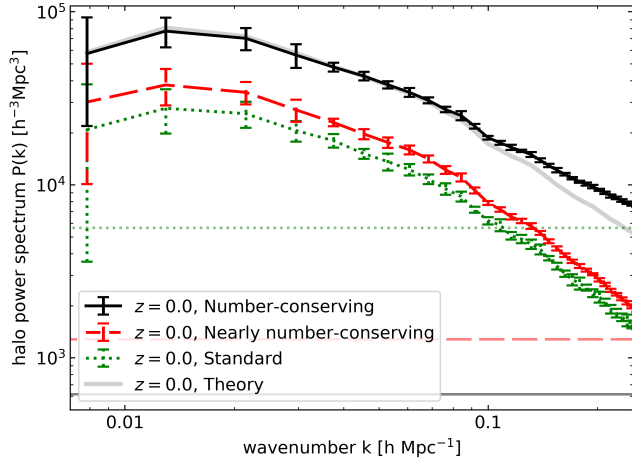


Figure 2. Power spectra at $z = 0$ of the halo samples shown in the dark gray band in Figure 1. Various curves show the power spectra of the halo samples at $z = 0$ evolved via the standard (dotted), the number-conserving (solid), and the nearly number-conserving (dashed) merger trees from the halo sample at z_* . The light gray curve (solid) shows the theoretical prediction at $z = 0$ of the Lagrangian perturbation theory based on the bias parameter of the halos at z_* . It matches the power spectrum of the halo sample (solid) following the number-conserving merger tree. Horizontal curves show the shot noises.

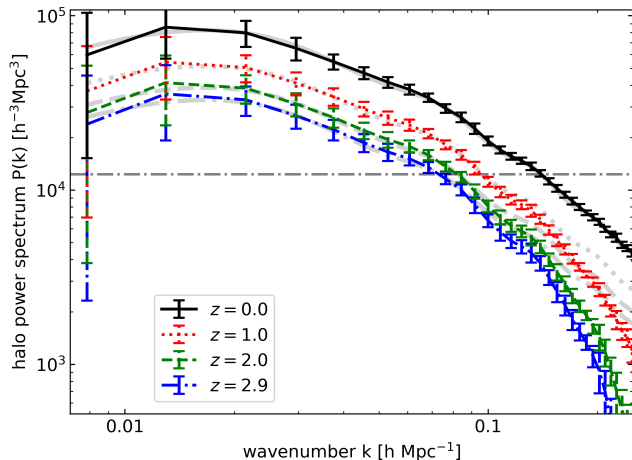


Figure 3. Power spectra at various redshifts of the halo sample shown in the light gray band in Figure 1 at $z = 0$. Various other curves show the power spectra of the halo sample at each redshift traced backward in time by considering those particles that belong to the same halo at $z = 0$ as a distinct halo at $z > 0$ and using the center-of-mass position as the position of the halo at $z > 0$. The gray curves show the theoretical predictions at each redshift of the Lagrangian perturbation theory based on the bias parameter of the halos at $z = 0$. They are in good agreement with the simulation results.

more halos separately identified at z_* could end up in the same halo at $z = 0$. In the number-conserving scheme, those in the same halo are all counted as individual halos

at the same position, while in the nearly number-conserving scheme this double counting is lifted (hence the number conservation is slightly violated).

For both cases (solid and dashed) the halos at z_* in the dark gray band are spread over a larger range of mass than in the standard merger tree (dotted). Certainly, many of those halos at z_* that disappear in the standard merger tree are part of massive halos at $z = 0$. For example, those halos at z_* comprise only 6% of the total mass in the histogram with $M \geq 10^{15} h^{-1} M_\odot$, but we keep their identities in these two merger trees. In particular, 52% of the halos at z_* are double counted at $z = 0$, shown as the difference between solid and dashed curves. The halo sample in the dark gray band at z_* maintains its identities in the solid curve at $z = 0$ with the number of halos conserved, and hence its evolution can be correctly modeled by the Lagrangian perturbation theory.

To answer the second question, we measure in Figure 2 the power spectra of three halo samples at $z = 0$ evolved from the same halo sample in the dark gray band at z_* , according to the standard (dotted), the number-conserving (solid), and the nearly number-conserving (dashed) merger trees. Compared to the standard merger tree, two other number-conserving trees have more halos in number, or lower shot noises. The distribution over halo mass in Figure 1 determines the bias of each halo sample, and the presence of more massive halos in the number-conserving merger tree boosts the halo power spectrum. Finally, the light gray curve is the theoretical prediction for the halo power spectrum at $z = 0$ from the halo sample in the dark gray band at z_* , where we used Equation (12) to predict $b_1(z = 0)$ by measuring $b_1(z_*)$ from simulations. The agreement of the theoretical prediction (gray) with the halo power spectrum (solid) from the number-conserving merger tree underpins that the number conservation is crucial in the Lagrangian perturbation theory for biased tracers. Mind that two other power spectra (dotted, dashed) without the number conservation are in significant disagreement with the theoretical prediction (gray).

In Figure 3 we test the significance of the number conservation in the standard approach to the Lagrangian perturbation theory for biased tracers. As shown in Figure 1, the halo sample at $z = 0$ originates from the particles that belong to various halos of widely different mass or from the particles unbound to any halos. Though those particles cannot be identified as physically distinct halos, we use the particle identification from the simulations to locate their positions at high redshifts and assign their center-of-mass positions to the positions of the halo sample at $z > 0$. Various curves in Figure 3 show the power spectra of the halo sample at $z > 0$. In the same way, we first measure the bias parameter from the halo sample at $z = 0$ and use Equation (12) to predict the bias parameters at high redshifts. The agreement of the theoretical predictions (gray) in the Lagrangian perturbation

theory with the simulation results once again confirms that the number conservation is crucial in the Lagrangian perturbation theory predictions. All the Figures are computed by averaging the halo samples from our ten simulations.

4. CONCLUSION AND DISCUSSION

The Lagrangian perturbation theory (Zel'dovich 1970; see, e.g., Buchert 1992; Bouchet et al. 1992; Buchert & Ehlers 1993; Buchert 1994; Bouchet et al. 1995; Catelan 1995; Bernardeau et al. 2002) is a very powerful tool for modeling the nonlinear matter power spectrum due to its simple analytical expression in Equation (1). Its applications to biased tracers such as dark matter halos and galaxies are widely popular for the same reason (see, e.g., Schneider & Bartelmann 1995; Taylor & Hamilton 1996; Matsubara 2008a), and the nonlinear power spectrum for biased tracers can be obtained from

$$\delta_h(\mathbf{k}, t) = \int d^3q e^{-i\mathbf{k}\cdot(\mathbf{q}+\Psi)} [1 + \delta_h(\mathbf{q}, t_i)] , \quad (13)$$

for $k > 0$. In this work, we have shown that the number conservation is crucial for the validity of this simple analytic expression for biased tracers. The number conservation is trivially satisfied for the evolution of dark matter particles, but biased tracers evolve through mergers and accretion of continuous matter.

By using numerical simulations and dark matter halos as our biased tracers, we have demonstrated that the Lagrangian perturbation theory prediction overestimates the halo power spectrum at $z = 0$ by a factor of 2.8 for a halo sample of mass $6 \times 10^{11} \leq M(h^{-1}M_\odot) < 2 \times 10^{12}$ defined at $z_* = 2.9$, if we trace their evolution according to the standard merger tree and hence the number conservation is violated. To demonstrate the significance of the number conservation, we have rectified the halo evolution by continuously tracing the individual halos from initial time until present, even if they merge into a larger halo and make up a tiny fraction of the merged halo. For the halo sample constructed this way, the number of halos stays constant throughout the evolution, and not surprisingly the Lagrangian perturbation theory prediction is in good agreement with the numerical simulation output.

Furthermore, we use the numerical simulations to test the significance of the number conservation in the standard approach to the Lagrangian perturbation theory. We chose a halo sample in a mass bin $5 \times 10^{13} \leq M(h^{-1}M_\odot) < 5 \times 10^{14}$ at $z = 0$ to trace backward in time the dark matter particles that belong to the halo sample. The particles in a given halo spread in space and become unbound to each other, as we move backward in time. By treating those particles as a distinct halo at $z > 0$, however, the number of halos is conserved throughout the backward evolution in the standard approach. Assigning the center-of-mass position of the particles to a halo position, we have demonstrated that

the Lagrangian perturbation theory predictions for the halo power spectrum at $z > 0$ match the numerical simulation results, as implemented in the standard approach to the Lagrangian perturbation theory.

As opposed to the case in numerical simulations, the halo number density $n_h(\mathbf{q}, t_i)$ or the fluctuation $\delta_h(\mathbf{q}, t_i)$ in Equation (13) is in practice not available in modeling the halo sample in the Eulerian frame. Real applications of the Lagrangian perturbation theory for biased tracers, however, involve marginalization of unknown bias parameters, rather than taking the bias parameters in the Lagrangian frame as input parameters. Hence the lack of information about those halos in the Lagrangian frame poses no real problem. Furthermore, as demonstrated in our numerical experiment, those bias parameters can be fixed from simulations as long as the number conservation is correctly imposed for those halos throughout the evolution.

In the Press-Schechter formalism (Press & Schechter 1974; Bardeen et al. 1986; Bond et al. 1991), the halo mass function at high redshift is used to compute the bias parameters in the Lagrangian space, and the bias parameter in the Eulerian space is then obtained by using Equations (10) and (12), under the assumption that the halo number is conserved (Mo & White 1996; Catelan et al. 1998; Sheth & Tormen 1999b; Bernardeau et al. 2002; Desjacques 2008; Matsubara 2008b, 2011; Carlson et al. 2013; White 2014; Matsubara & Desjacques 2016; Desjacques et al. 2018). With halos physically identifiable at high z as counted in the halo mass function in the Press-Schechter formalism, their physical evolution would be similar to those in our standard merger tree, as halos evolve through mergers and accretion, violating the number conservation. Hence, the predictions for the Eulerian bias parameters made in the Press-Schechter formalism with the number conservation should then correspond to the halo samples in our number-conserving merger tree.

Recent modeling of biased tracers in the Lagrangian perturbation theory includes higher-order bias parameters such as b_2 , the tidal bias b_{s^2} , and so on. These bias parameters are associated with the corresponding higher-order operators $\mathcal{O}(\mathbf{q}) \ni \delta^2, s^2$, which are often described in the field-level models. Furthermore, it was recently shown (Vlah et al. 2016; Schmittfull et al. 2019; Chen et al. 2020; Schmidt 2021) that the field-level modeling of biased tracers in fact works extremely well. With large degree of freedom in the bias parameters, cosmological parameters are successfully extracted (Nishimichi et al. 2020; d'Amico et al. 2020; Ivanov et al. 2020; Chen et al. 2021) after marginalizing over bias parameters.

In the field-level modeling, Equation (13) yields that the halo number density fluctuation $\delta_h(\mathbf{q}, t_i)$ in the Eulerian frame is described in terms of operators $\tilde{\mathcal{O}}_i(\mathbf{x}, t)$ in the Eule-

rian frame for each arbitrary bias parameter, where

$$\tilde{\mathcal{O}}_i(\mathbf{k}, t) := \int d^3q \mathcal{O}_i(\mathbf{q}) e^{-i\mathbf{k}\cdot(\mathbf{q}+\Psi)}. \quad (14)$$

These are called the *shifted* operators, as the computations in the field-level models start with operators $\mathcal{O}_i(\mathbf{q})$ in the Lagrangian frame by shifting them to the Eulerian frame $\tilde{\mathcal{O}}_i(\mathbf{x}, t)$ according to the displacement field (a.k.a. shifted operators). Given a series of shifted operators, halos are then modeled with arbitrary bias parameters, which in the end amounts to the effective field theory approach in the Eulerian frame (Mirbabayi et al. 2015; Senatore 2015; Vlah et al. 2015b; Ivanov et al. 2020) (but of course with different operators).

However, without the number conservation of any field associated with each operator \mathcal{O}_i , the shifted operator in Equation (14) is not the Fourier transform of the field evolved from $\mathcal{O}_i(\mathbf{q})$ in the Lagrangian frame. In other words, this proce-

dure of shifting an operator $\mathcal{O}_i(\mathbf{q})$ in the Lagrangian space to Eulerian space by using $\mathbf{x} = \mathbf{q} + \Psi$ is not equivalent to Equation (14). The notation here is again a misnomer in a sense that $n_h(\mathbf{q}, t_i)$ represents not physical halos at t_i , but the particle distribution at t_i that eventually form halos in the Eulerian frame. Hence, this procedure works just fine, because in the end $\tilde{\mathcal{O}}_i(\mathbf{k}, t)$ is some operator in the Eulerian space defined in terms of $\mathcal{O}_i(\mathbf{q})$ in the Lagrangian space with large-scale bulk motion accounted for. But it is clear that two fields $\mathcal{O}_i(\mathbf{q})$ and $\mathcal{O}_i(\mathbf{x}, t)$ are not related.

ACKNOWLEDGMENTS

We acknowledge useful discussions with Julian Adamek, Andrej Obuljen, and Zvonimir Vlah. This work is supported by the Swiss National Science Foundation Grant CR-SII5_198674. We acknowledge access to Piz Daint and Alps at the Swiss National Supercomputing Centre under the project ID UZH-24.

REFERENCES

- Baldauf, T., Seljak, U., Desjacques, V., & McDonald, P. 2012, *PhRvD*, 86, 083540, doi: [10.1103/PhysRevD.86.083540](https://doi.org/10.1103/PhysRevD.86.083540)
- Bardeen, J. M., Bond, J. R., Kaiser, N., & Szalay, A. S. 1986, *ApJ*, 304, 15, doi: [10.1086/164143](https://doi.org/10.1086/164143)
- Benson, A. J., Cole, S., Frenk, C. S., Baugh, C. M., & Lacey, C. G. 2000, *MNRAS*, 311, 793, doi: [10.1046/j.1365-8711.2000.03101.x](https://doi.org/10.1046/j.1365-8711.2000.03101.x)
- Bernardeau, F., Colombi, S., Gaztañaga, E., & Scoccimarro, R. 2002, *PhR*, 367, 1, doi: [10.1016/S0370-1573\(02\)00135-7](https://doi.org/10.1016/S0370-1573(02)00135-7)
- Blas, D., Lesgourgues, J., & Tram, T. 2011, *JCAP*, 2011, 034, doi: [10.1088/1475-7516/2011/07/034](https://doi.org/10.1088/1475-7516/2011/07/034)
- Bond, J. R., Cole, S., Efstathiou, G., & Kaiser, N. 1991, *ApJ*, 379, 440
- Bouchet, F. R., Colombi, S., Hivon, E., & Juszkiewicz, R. 1995, *A&A*, 296, 575, doi: [10.48550/arXiv.astro-ph/9406013](https://doi.org/10.48550/arXiv.astro-ph/9406013)
- Bouchet, F. R., Juszkiewicz, R., Colombi, S., & Pellat, R. 1992, *ApJL*, 394, L5, doi: [10.1086/186459](https://doi.org/10.1086/186459)
- Brammer, G. B., Whitaker, K. E., van Dokkum, P. G., et al. 2011, *ApJ*, 739, 24, doi: [10.1088/0004-637X/739/1/24](https://doi.org/10.1088/0004-637X/739/1/24)
- Buchert, T. 1992, *MNRAS*, 254, 729, doi: [10.1093/mnras/254.4.729](https://doi.org/10.1093/mnras/254.4.729)
- . 1994, *MNRAS*, 267, 811, doi: [10.1093/mnras/267.4.811](https://doi.org/10.1093/mnras/267.4.811)
- Buchert, T., & Ehlers, J. 1993, *MNRAS*, 264, 375, doi: [10.1093/mnras/264.2.375](https://doi.org/10.1093/mnras/264.2.375)
- Carlson, J., Reid, B., & White, M. 2013, *MNRAS*, 429, 1674, doi: [10.1093/mnras/sts457](https://doi.org/10.1093/mnras/sts457)
- Catelan, P. 1995, *MNRAS*, 276, 115, doi: [10.1093/mnras/276.1.115](https://doi.org/10.1093/mnras/276.1.115)
- Catelan, P., Lucchin, F., Matarrese, S., & Porciani, C. 1998, *MNRAS*, 297, 692
- Catelan, P., Porciani, C., & Kamionkowski, M. 2000, *MNRAS*, 318, L39, doi: [10.1046/j.1365-8711.2000.04023.x](https://doi.org/10.1046/j.1365-8711.2000.04023.x)
- Chen, S.-F., Vlah, Z., Castorina, E., & White, M. 2021, *JCAP*, 2021, 100, doi: [10.1088/1475-7516/2021/03/100](https://doi.org/10.1088/1475-7516/2021/03/100)
- Chen, S.-F., Vlah, Z., & White, M. 2020, *JCAP*, 2020, 062, doi: [10.1088/1475-7516/2020/07/062](https://doi.org/10.1088/1475-7516/2020/07/062)
- Conselice, C. J., Wilkinson, A., Duncan, K., & Mortlock, A. 2016, *ApJ*, 830, 83, doi: [10.3847/0004-637X/830/2/83](https://doi.org/10.3847/0004-637X/830/2/83)
- Crocce, M., & Scoccimarro, R. 2006, *PhRvD*, 73, 063519, doi: [10.1103/PhysRevD.73.063519](https://doi.org/10.1103/PhysRevD.73.063519)
- Croton, D. J., Springel, V., White, S. D. M., et al. 2006, *MNRAS*, 365, 11, doi: [10.1111/j.1365-2966.2005.09675.x](https://doi.org/10.1111/j.1365-2966.2005.09675.x)
- d’Amico, G., Gleyzes, J., Kokron, N., et al. 2020, *JCAP*, 2020, 005, doi: [10.1088/1475-7516/2020/05/005](https://doi.org/10.1088/1475-7516/2020/05/005)
- Davis, M., Efstathiou, G., Frenk, C. S., & White, S. D. M. 1985, *ApJ*, 292, 371, doi: [10.1086/163168](https://doi.org/10.1086/163168)
- Desjacques, V. 2008, *PhRvD*, 78, 103503, doi: [10.1103/PhysRevD.78.103503](https://doi.org/10.1103/PhysRevD.78.103503)
- Desjacques, V., Jeong, D., & Schmidt, F. 2018, *PhR*, 733, 1, doi: [10.1016/j.physrep.2017.12.002](https://doi.org/10.1016/j.physrep.2017.12.002)
- Eisenstein, D. J., Annis, J., Gunn, J. E., et al. 2001, *AJ*, 122, 2267, doi: [10.1086/323717](https://doi.org/10.1086/323717)
- Fry, J. N. 1996, *ApJL*, 461, L65, doi: [10.1086/310006](https://doi.org/10.1086/310006)
- Fry, J. N., & Gaztanaga, E. 1993, *ApJ*, 413, 447, doi: [10.1086/173015](https://doi.org/10.1086/173015)
- Hand, N., Feng, Y., Beutler, F., et al. 2018, *AJ*, 156, 160, doi: [10.3847/1538-3881/aadae0](https://doi.org/10.3847/1538-3881/aadae0)
- Ivanov, M. M., Simonović, M., & Zaldarriaga, M. 2020, *JCAP*, 2020, 042, doi: [10.1088/1475-7516/2020/05/042](https://doi.org/10.1088/1475-7516/2020/05/042)

- Kauffmann, G., Colberg, J. M., Diaferio, A., & White, S. D. M. 1999, *MNRAS*, 303, 188, doi: [10.1046/j.1365-8711.1999.02202.x](https://doi.org/10.1046/j.1365-8711.1999.02202.x)
- Ma, C.-P., & Fry, J. N. 2000, *ApJ*, 543, 503, doi: [10.1086/317146](https://doi.org/10.1086/317146)
- Matsubara, T. 2008a, *PhRvD*, 77, 063530, doi: [10.1103/PhysRevD.77.063530](https://doi.org/10.1103/PhysRevD.77.063530)
- . 2008b, *PhRvD*, 78, 083519, doi: [10.1103/PhysRevD.78.083519](https://doi.org/10.1103/PhysRevD.78.083519)
- . 2011, *PhRvD*, 83, 083518, doi: [10.1103/PhysRevD.83.083518](https://doi.org/10.1103/PhysRevD.83.083518)
- Matsubara, T., & Desjacques, V. 2016, *PhRvD*, 93, 123522, doi: [10.1103/PhysRevD.93.123522](https://doi.org/10.1103/PhysRevD.93.123522)
- McDonald, P., & Vlah, Z. 2018, *PhRvD*, 97, 023508, doi: [10.1103/PhysRevD.97.023508](https://doi.org/10.1103/PhysRevD.97.023508)
- Mirbabayi, M., Schmidt, F., & Zaldarriaga, M. 2015, *JCAP*, 2015, 030, doi: [10.1088/1475-7516/2015/07/030](https://doi.org/10.1088/1475-7516/2015/07/030)
- Mo, H. J., & White, S. D. M. 1996, *MNRAS*, 282, 347
- Nishimichi, T., D'Amico, G., Ivanov, M. M., et al. 2020, *PhRvD*, 102, 123541, doi: [10.1103/PhysRevD.102.123541](https://doi.org/10.1103/PhysRevD.102.123541)
- Padmanabhan, N., & White, M. 2009, *PhRvD*, 80, 063508, doi: [10.1103/PhysRevD.80.063508](https://doi.org/10.1103/PhysRevD.80.063508)
- Pietroni, M. 2018, *JCAP*, 2018, 028, doi: [10.1088/1475-7516/2018/06/028](https://doi.org/10.1088/1475-7516/2018/06/028)
- PLANCK Collaboration. 2020, *A&A*, 641, A1, doi: [10.1051/0004-6361/201833880](https://doi.org/10.1051/0004-6361/201833880)
- Potter, D., Stadel, J., & Teyssier, R. 2017, *CompAC*, 4, 2, doi: [10.1186/s40668-017-0021-1](https://doi.org/10.1186/s40668-017-0021-1)
- Press, W. H., & Schechter, P. 1974, *ApJ*, 187, 425
- Rampf, C., Frisch, U., & Hahn, O. 2021, *MNRAS*, 505, L90, doi: [10.1093/mnras/505/1/90](https://doi.org/10.1093/mnras/505/1/90)
- Schmidt, F. 2021, *JCAP*, 2021, 033, doi: [10.1088/1475-7516/2021/04/033](https://doi.org/10.1088/1475-7516/2021/04/033)
- Schmittfull, M., Simonović, M., Assassi, V., & Zaldarriaga, M. 2019, *PhRvD*, 100, 043514, doi: [10.1103/PhysRevD.100.043514](https://doi.org/10.1103/PhysRevD.100.043514)
- Schneider, P., & Bartelmann, M. 1995, *MNRAS*, 273, 475, doi: [10.1093/mnras/273.2.475](https://doi.org/10.1093/mnras/273.2.475)
- Senatore, L. 2015, *JCAP*, 2015, 007, doi: [10.1088/1475-7516/2015/11/007](https://doi.org/10.1088/1475-7516/2015/11/007)
- Sheth, R. K., & Tormen, G. 1999a, *MNRAS*, 308, 119, doi: [10.1046/j.1365-8711.1999.02692.x](https://doi.org/10.1046/j.1365-8711.1999.02692.x)
- . 1999b, *MNRAS*, 308, 119
- Springel, V., White, S. D. M., Tormen, G., & Kauffmann, G. 2001, *MNRAS*, 328, 726, doi: [10.1046/j.1365-8711.2001.04912.x](https://doi.org/10.1046/j.1365-8711.2001.04912.x)
- Szalay, A. S. 1988, *ApJ*, 333, 21, doi: [10.1086/166721](https://doi.org/10.1086/166721)
- Taruya, A., & Colombi, S. 2017, *MNRAS*, 470, 4858, doi: [10.1093/mnras/stx1501](https://doi.org/10.1093/mnras/stx1501)
- Taylor, A. N., & Hamilton, A. J. S. 1996, *MNRAS*, 282, 767, doi: [10.1093/mnras/282.3.767](https://doi.org/10.1093/mnras/282.3.767)
- Tegmark, M., & Peebles, P. J. E. 1998, *ApJL*, 500, L79
- Tinker, J., Kravtsov, A. V., Klypin, A., et al. 2008, *ApJ*, 688, 709, doi: [10.1086/591439](https://doi.org/10.1086/591439)
- Tinker, J. L., Robertson, B. E., Kravtsov, A. V., et al. 2010, *ApJ*, 724, 878, doi: [10.1088/0004-637X/724/2/878](https://doi.org/10.1088/0004-637X/724/2/878)
- Vlah, Z., Castorina, E., & White, M. 2016, *JCAP*, 2016, 007, doi: [10.1088/1475-7516/2016/12/007](https://doi.org/10.1088/1475-7516/2016/12/007)
- Vlah, Z., Seljak, U., & Baldauf, T. 2015a, *PhRvD*, 91, 023508, doi: [10.1103/PhysRevD.91.023508](https://doi.org/10.1103/PhysRevD.91.023508)
- Vlah, Z., White, M., & Aviles, A. 2015b, *JCAP*, 2015, 014, doi: [10.1088/1475-7516/2015/09/014](https://doi.org/10.1088/1475-7516/2015/09/014)
- White, M. 2014, *MNRAS*, 439, 3630, doi: [10.1093/mnras/stu209](https://doi.org/10.1093/mnras/stu209)
- White, Blanton, Bolton, Schlegel, Tinker, Berlind, da Costa, Kazin, Lin, Maia, McBride, Padmanabhan, Parejko, Percival, Prada, Ramos, Sheldon, de Simoni, Skibba, Thomas, Wake, Zehavi, Zheng, Nichol, Schneider, Strauss, Weaver, & Weinberg, 2011, *ApJ*, 728, 126, doi: [10.1088/0004-637X/728/2/126](https://doi.org/10.1088/0004-637X/728/2/126)
- Zel'dovich, Y. B. 1970, *A&A*, 5, 84